The $N\bar{N}$ interaction in a constituent quark model: Baryonium states and protonium level shifts

D. R. Entem and F. Fernández
Grupo de Física Nuclear, IUFFyM, Universidad de Salamanca, E-37008 Salamanca, Spain
(Received 15 February 2006; published 28 April 2006)

We derive a $N\bar{N}$ interaction from a constituent quark model constrained by the NN sector to investigate the possible baryonium resonant state $X(1835)$ recently suggested as a possible interpretation of the near-threshold enhancement found in $J/\psi \to \gamma p\bar{p}$ by the BES Collaboration. The interaction does not show bound or quasibound states but a $^3P_0$ resonance in the $I = 0$ isospin channel. We analyze the shift of the antiprotonium hydrogen energy levels, finding that $p\bar{p}$-$n\bar{n}$ mixing can explain the abnormally big value of the $2\,^3P_0$ energy shift.

DOI: 10.1103/PhysRevC.73.045214 PACS number(s): 12.39.Jh, 13.75.Cs, 25.43.+t, 21.10.Dr

I. INTRODUCTION

The recent observation of a near-threshold narrow enhancement in the $p\bar{p}$ invariant mass spectrum from radiative $J/\psi \to \gamma p\bar{p}$ decay by the BES Collaboration [1] has renewed interest in the $N\bar{N}$ interaction and its possible baryonium bound states. If this enhancement is fitted with an S-wave Breit-Wigner resonance function the resulting peak mass is $M = 1859 \pm 6$ MeV, which is below the $p\bar{p}$ threshold, whereas a P-wave fit gives a peak mass very close to the threshold at $M = 1876 \pm 0.9$ MeV. The photon polar angle distribution is consistent with $1 + \cos^2\theta$, which suggests that the total angular momentum is very likely to be $J = 0$. So this structure may have quantum numbers $J^{PC} = 0^{-+}$ or $J^{PC} = 0^{++}$, which, in principle, do not correspond to any known meson resonance. However, no similar signal was observed by BES in the $\pi^0 p\bar{p}$ channel, which suggests that the enhancement is due to an isoscalar resonance.

The simplest interpretation of the experimental $J/\psi \to \gamma p\bar{p}$ is a baryonium bound state [2], although the result is currently being interpreted in several ways [3–6].

The study of the possible nucleon-antinucleon bound states has a very long history (see Ref. [7] and references therein). Usually, the real part of the $N\bar{N}$ interaction is derived by G-parity transformation of the NN potentials [7]. However, this recipe cannot be straightforwardly applied to the short-range part because in most of the NN potentials this part of the interaction is described phenomenologically [7], ignoring quark degrees of freedom, which should be relevant at this scale.

Naturally, the $N\bar{N}$ potential obtained in that way is not the whole story. The derivation of the annihilation part is still a major challenge. Attempts have been made to construct the annihilation potential in coupled-channel models in terms of quark rearrangement or baryon exchanges [7], but the best results are still obtained by resorting to phenomenological treatments. Perhaps the simplest possibility is adding ad hoc an imaginary part to the meson exchange model [8]. Although, as showed by Myhrer and Thomas [9], part of the bound-state spectrum produced by the real part may be washed out when annihilation is taken into account, most of the meson-exchange-based potentials, like the Paris or Bonn potentials, predict more than one quasibound state mainly in S waves.

A different approach is the one that relies on the quark structure of hadrons. In quark-based NN interactions part of the short-range repulsion comes from the antisymmetry between quarks. This fact has important consequences on the $N\bar{N}$ potentials as compared, for example, with the conventional one-boson exchange models. In the meson-exchange picture the central force is provided basically by the σ and the ω. They have opposite sign for the NN system but add coherently in the $N\bar{N}$. Moreover, the spin-orbit force coming from these two exchanges adds in NN and cancels in $N\bar{N}$. The ω-exchange contribution is replaced in quark-based models by the antisymmetry, which is not present in $N\bar{N}$. Therefore quark-based $N\bar{N}$ potentials may look different from the conventional ones. Furthermore, the NN one-pion-exchange tensor interaction is attenuated also by antisymetrization and not by ρ exchanges. This fact, which has observable consequences at the NN level [10], may also significantly change the whole $N\bar{N}$ interaction. Therefore it would be desirable to have $N\bar{N}$ potentials derived from quark degrees of freedom to check whether baryonium bound states appear.

Among the different quark approaches, the constituent quark model developed in Ref. [11] may be indicated for this purpose. It has been shown that this model is successful in describing deuteron properties, NN phase shifts, and hadron phenomenology [11,12].

We will apply this model to study two topics in low-energy antiproton physics: the possible bound states or near-threshold resonances in $p\bar{p}$ scattering and the energy level shifts in protonium. To do that we will use a $N\bar{N}$ potential derived by G-parity transformation of the quark-model-based NN interaction of Ref. [11]. Annihilation is taken into account by a complex interaction being the real part generated by one-pion and one-gluon exchange annihilation and taking the imaginary part as an energy-independent potential of Gaussian form. In this way all the parameters of the interaction are constrained by the NN sector except the two parameters describing the imaginary potential.

The paper is organized as follows. After this introduction in Sec. II we explain the basis of our model. Section III is devoted to the development of the $N\bar{N}$ interaction. The results for the $N\bar{N}$ cross section and phase shits are presented in Sec. IV and the possible bound states are discussed. Section V is devoted

to a possible explanation of experimental values of the energy shifts in protonium. The paper ends with some concluding remarks.

II. THE MODEL

Constituent quark models are based on the assumption that the constituent quark mass is generated by the spontaneous breaking of the original $SU(3)_L \otimes SU(3)_R$ symmetry of the QCD Lagrangian for (almost) massless quarks at some momentum scale [13].

The picture of the QCD vacuum as a dilute medium of instantons [14] explains nicely such symmetry breaking, which is the most important nonperturbative phenomenon for hadron structure at low energies. Quarks interact with fermionic zero modes of the individual instantons in the medium and therefore the light quark propagator gets modified, acquiring a momentum-dependent mass that drops to zero for momentum lighter than the inverse of the average instanton size $\bar{\rho}$.

The momentum-dependent mass acts as a natural cutoff of the theory. In the domain of momentum $k < 1/\bar{\rho}$ a simple Lagrangian invariant under chiral transformations can be derived as [14]

$$\mathcal{L} = \bar{\psi}(i\gamma^\mu \partial_\mu - M U^{\gamma_5})\psi, \tag{1}$$

where $U^{\gamma_5} = \exp(i\pi^a \lambda^a \gamma_5 / f_\pi)$, π^a denotes the pseudoscalar fields $(\vec{\pi}, K_i, \eta_8)$ with $i = 1, \ldots, 4$, and M is the constituent quark mass. An expression for the constituent quark mass can be obtained from the theory, but it also can be parametrized as $M(q^2) = m_q F(q^2)$ with

$$F(q^2) = \left[\frac{\Lambda^2}{\Lambda^2 + q^2}\right]^{1/2}, \tag{2}$$

where Λ determines the chiral symmetry-breaking scale.

The matrix U^{γ_5} can be expanded in terms of basic fields as

$$U^{\gamma_5} = 1 + \frac{i}{f_\pi}\gamma_5 \lambda^a \pi^a - \frac{1}{2f_\pi^2}\pi^a \pi^a + \ldots. \tag{3}$$

The first term generates the constituent quark mass and the second one gives rise to the one boson exchange interactions between quarks. The main contribution of the third term comes from the correlated two-pion exchanges, which can be simulated by means of the one-sigma exchange potential [15].

Beyond the chiral symmetry-breaking scale one expects the dynamics to be governed by QCD perturbative effects. There are consequences of the one-gluon fluctuations around the instanton vacuum and we take it into account through the qqg coupling

$$\mathcal{L}_{gqq} = i\sqrt{4\pi}\alpha_s \bar{\psi}\gamma_\mu G_c^\mu \lambda^c \psi, \tag{4}$$

where λ^c are the SU(3) color matrices and G_c^μ is the gluon field. Since any quark-antiquark exchange between N and $\bar{N}$ is not allowed, the $N\bar{N}$ interaction from one-gluon exchange is very different from the NN one. As the gluon carries color, it cannot be exchanged between colorless states and only contributes through annihilation diagrams. The next non-zero contribution will be the color singlet part of the two-gluon exchange. This has been considered in the $N\bar{N}$ system [16] and has been shown to be important in the η-nucleon systems [17]. There are two main reasons why we do not include this contribution. First, owing to our value of α_s, the contribution will be reduced by 50%. Second, as we will see in the following, the one-pion exchange contribution dominates the dynamics of the $N\bar{N}$ system.

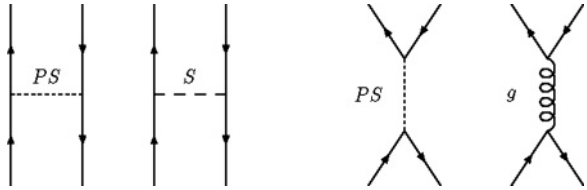

FIG. 1. Diagrams that contributes to the microscopic $q\bar{q}$ interaction.

Finally, one should incorporate another nonperturbative effect, namely the confinement. Such a term can be physically interpreted in a picture in which the quark and the antiquark are linked by a one-dimensional color flux tube. The spontaneous creation of light-quark pairs may give rise to a breakup of the color flux tube. This can be translated into a screened potential [18] in such a way that the potential saturates at the same interquark distance. This potential necessary to describe hadron structure does not contribute to the $N\bar{N}$ interaction but guarentees that N and $\bar{N}$ do not collapse under the interaction just described.

The nonrelativistic reductions of such interactions are given in [11] and have been used to study the NN system. All the parameters appearing in the aforementioned potentials are fixed in the NN sector.

To get the $q\bar{q}$ interaction we have to perform a G-parity transformation of the qq potentials. As already explained only pseudoscalar and scalar boson exchanges are relevant. The reason is that when one calculates the $N\bar{N}$ interaction from the $q\bar{q}$ interaction there are no exchange diagrams as in the NN case.

Once the G-parity transformation is performed we get

$$V_{q\bar{q}}^{\mathrm{PS}}(\vec{q}) = \frac{1}{(2\pi)^3}\frac{g_{\mathrm{ch}}^2}{4m_q^2}\frac{\Lambda_{\chi\mathrm{SB}}^2}{\Lambda_{\chi\mathrm{SB}}^2 + q^2}\frac{(\vec{\sigma}_i \cdot \vec{q})(\vec{\sigma}_j \cdot \vec{q})}{m_{\mathrm{PS}}^2 + q^2}(\vec{\tau}_i \cdot \vec{\tau}_j), \tag{5}$$

$$V_{q\bar{q}}^{S}(\vec{q}) = -\frac{g_{\mathrm{ch}}^2}{(2\pi)^3}\frac{\Lambda_{\chi\mathrm{SB}}^2}{\Lambda_{\chi\mathrm{SB}}^2 + q^2}\frac{1}{m_S^2 + q^2}, \tag{6}$$

which are the first two diagrams in Fig. 1.

In the $q\bar{q}$ system there are also annihilation contributions. These are the second pair of diagrams in Fig. 1. The real part of this potential can be derived in our model by annihilation diagrams of the one-gluon and one-pion exchange. This interaction in momentum representation can be written as [19]

$$V_{q\bar{q}}^{\mathrm{A,PS}}(\vec{q}) = \frac{1}{(2\pi)^3}\frac{g_{\mathrm{ch}}^2}{4m_q^2 - m_{\mathrm{PS}}^2}\left(\frac{1}{3} + \frac{1}{2}\vec{\lambda}_1 \cdot \vec{\lambda}_2\right) \times \left(\frac{1}{2} - \frac{1}{2}\vec{\sigma}_1 \cdot \vec{\sigma}_2\right)\left(\frac{3}{2} + \frac{1}{2}\vec{\tau}_1 \cdot \vec{\tau}_2\right), \tag{7}$$

$$V_{q\bar{q}}^{\mathrm{A,OGE}}(\vec{q}) = \frac{1}{(2\pi)^3} 4\pi \frac{\alpha_s}{4m_q^2} \left(\frac{4}{9} - \frac{1}{12}\vec{\lambda}_1 \cdot \vec{\lambda}_2\right) \times \left(\frac{3}{2} + \frac{1}{2}\vec{\sigma}_1 \cdot \vec{\sigma}_2\right)\left(\frac{1}{2} - \frac{1}{2}\vec{\tau}_1 \cdot \vec{\tau}_2\right), \quad (8)$$

the first one coming from annihilation through a pseudoscalar boson and the second one through a gluon.

III. THE $N\bar{N}$ INTERACTION

Once the microscopic model is fixed we use the resonating group method to derive the $N\bar{N}$ interaction in the same way as we did in the *NN* case. The wave functions for the baryon (antibaryon) states are

$$\psi_B = \phi_B(\vec{p}_{\xi_1}, \vec{p}_{\xi_2})\chi_B\xi_c[1^3], \quad (9)$$

where χ_B is the spin-isospin wave function, ξ_c is the color wave function, and

$$\phi_B(\vec{p}_{\xi_1}, \vec{p}_{\xi_2}) = \left[\frac{2b^2}{\pi}\right]^{\frac{3}{4}} e^{-b^2 p_{\xi_1}^2} \left[\frac{3b^2}{2\pi}\right]^{\frac{3}{4}} e^{-\frac{3b^2}{4} p_{\xi_2}^2} \quad (10)$$

is the orbital wave function, with b the parameter related to the size of the baryon (antibaryon) and $\vec{p}_{\xi_1}, \vec{p}_{\xi_2}$ the Jacobi momenta of the baryons.

The N and $\bar{N}$ wave functions are the same provided that we relate the spin-isospin part by G-parity.

As already mentioned, only direct diagrams contribute to the $N\bar{N}$ potential. These are shown in Fig. 2. For the first diagram we calculate the interaction as in the *NN* case but without exchange diagrams. It is interesting to note that, since no exchange diagram is present, the interaction is local and from the orbital part we only get a form factor.

For the $N\bar{N}$ annihilation potential corresponding to the second diagram in Fig. 2 we get

$$V_{N\bar{N}}^{\mathrm{Anh}}(\vec{q}) = V_{\mathrm{SI}}\, e^{-\frac{q^2 b^2}{3}}, \quad (11)$$

where V_{SI} for the pion is

$$V_{\mathrm{SI}}^{\mathrm{PS}} = \frac{g_{\mathrm{ch}}^2}{(2\pi)^3} \frac{1}{4m_q^2 - m_{\mathrm{PS}}^2} \frac{1}{108}(243 - 27\,\vec{\sigma}_N \cdot \vec{\sigma}_{\bar{N}} + 9\vec{\tau}_N \cdot \vec{\tau}_{\bar{N}} - 25\vec{\sigma}_N \cdot \vec{\sigma}_{\bar{N}}\, \vec{\tau}_N \cdot \vec{\tau}_{\bar{N}}) \quad (12)$$

and that for the gluon is

$$V_{\mathrm{SI}}^{\mathrm{OGE}} = \frac{1}{2\pi^2} \frac{\alpha_s}{81} \frac{1}{4m_q^2}(243 + 9\,\vec{\sigma}_N \cdot \vec{\sigma}_{\bar{N}} - 27\vec{\tau}_N \cdot \vec{\tau}_{\bar{N}} - 25\vec{\sigma}_N \cdot \vec{\sigma}_{\bar{N}}\, \vec{\tau}_N \cdot \vec{\tau}_{\bar{N}}). \quad (13)$$

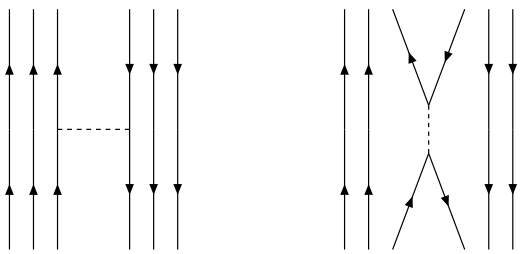

FIG. 2. Diagrams that contributes to the $N\bar{N}$ potential.

TABLE I. Quark-model parameters.

m_q(MeV)	313
b(fm)	0.518
α_s	0.497
g_{ch}^2	6.66
m_S(fm^{-1})	3.513
m_{PS}(fm^{-1})	0.70
$\Lambda_{\chi\mathrm{SB}}$(fm^{-1})	4.29
b'(fm)	0.848
W_i(GeV^{-2})	−0.74

To have a realistic model it is important to include the annihilation into mesons. Annihilation processes are very complicated; for a review see [20]. There are microscopic models at quark level that describe such processes. Usually these models are highly non-local and energy dependent, and instead of using one of these, we chose to describe such processes with an optical potential to simplify the calculation. This approximation was already used by Bryan and Phillips [21], Dover and Richard [22], and Kohno and Weise [23]. They all used a similar parametrization but as the real part of the $N\bar{N}$ was different they obtained different potentials. We chose to use a parametrization similar to the one used in [24] but we do not allow a spin or isospin dependence, so

$$V_{q\bar{q}}^{\mathrm{Anh}}(\vec{q}) = i\, W_i\, e^{-\frac{q^2 b'^2}{3}}, \quad (14)$$

where W_i gives the strength and b' the range.

The parameters of the model are presented in Table I. All but the last two parameters are fixed from the *NN* sector using the same set as in [11]. To fix b' and W_i we use the total annihilation cross section for the $p\bar{p}$ system. We calculate this cross section by solving the Lippmann-Schwinger equation in each partial wave with the complex potential discussed previously. The partial waves for the $N\bar{N}$ system are almost the same as in the *NN* case. The only difference is due to the symmetry requirement in the second case that fixes the isospin in each partial wave. For the $N\bar{N}$ system all partial waves can have isospin 0 or 1. For each total angular momentum J and isospin I we have the singlet state $S = 0$ and $L = J$ and the triplet states $S = 1$, one of them uncoupled, $L = J$, and the other two coupled, $L = J - 1, J + 1$.

The scattering cross section is given in terms of the scattering matrix elements in each partial wave. We denote the singlet matrix element as ${}^0S_J^{JI}$, the uncoupled triplet as ${}^3S_J^{JI}$, the diagonal matrix elements for the coupled triplet as ${}^3S_{J\pm1}^{JI}$, and the nondiagonal matrix elements as ${}^3S_{J\pm1,J\mp1}^{JI}$. With this notation the annihilation cross section is given by

$$\sigma_A^I = \frac{\pi}{4p^2} \sum_J (2J+1)\left[\left(1 - \left|{}^0S_J^{JI}\right|^2\right) + \left(1 - \left|{}^3S_J^{JI}\right|^2\right) + \left(2 - \left|{}^3S_{J+1}^{JI}\right|^2 - \left|{}^3S_{J-1}^{JI}\right|^2 - 2\left|{}^3S_{J+1,J-1}^{JI}\right|^2\right)\right] \quad (15)$$

in each isospin channel I. Of course the second line is not present for $J = 0$ since only the singlet and uncoupled triplet

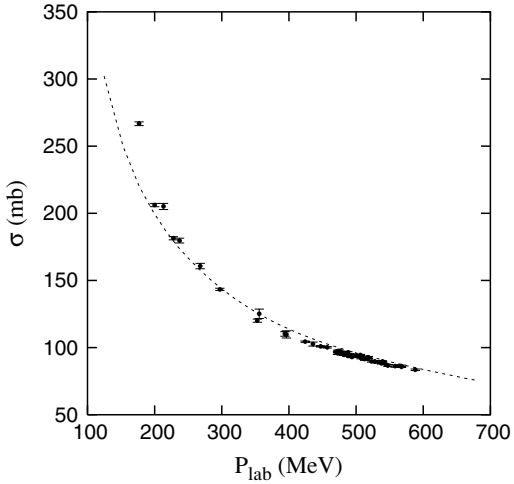

FIG. 3. $p\bar{p}$ annihilation cross section. Experimental data are from Ref. [22].

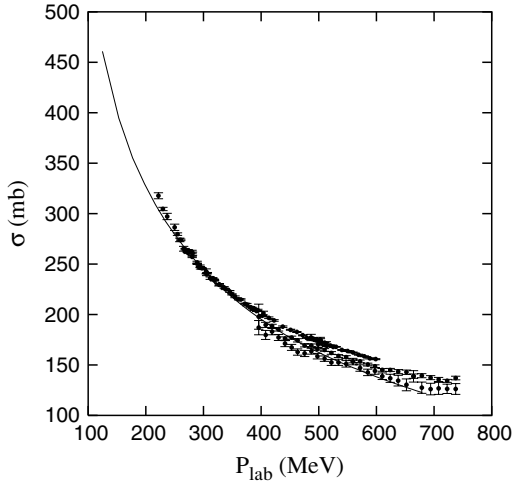

FIG. 4. $p\bar{p}$ total cross section. Experimental data are from Refs. [26–29].

states are possible. The $p\bar{p}$ cross section is

$$\sigma_A^{p\bar{p}} = \tfrac{1}{2}\left(\sigma_A^0 + \sigma_A^1\right), \tag{16}$$

since $p\bar{p}$ is a linear combination of isospin 0 and 1 states.

The imaginary part of the potential dominates this annihilation cross section and we use this cross section to fix the two parameters of Eq. (14). With these two parameters we are able to fit the annihilation data in the laboratory momentum range between 100 and 600 MeV as shown in Fig. 3.

IV. RESULTS: CROSS SECTIONS AND BOUND STATES

Once the annihilation cross section is fitted, we calculate the elastic cross section by

$$\sigma_e^I = \frac{\pi}{4p^2}\sum_J (2J+1)\Big[\left|1 - {}^0S_J^{JI}\right|^2 + \left|1 - {}^3S_J^{JI}\right|^2 + \left|1 - {}^3S_{J+1}^{JI}\right|^2 + \left|1 - {}^3S_{J-1}^{JI}\right|^2 + 2\left|{}^3S_{J+1,J-1}^{JI}\right|^2\Big] \tag{17}$$

in each isospin channel I. In the $p\bar{p}$ channel the sum of the elastic and charge exchange reaction cross sections is

$$\sigma_e^{p\bar{p}} + \sigma_{ce}^{p\bar{p}} = \tfrac{1}{2}\left(\sigma_e^0 + \sigma_e^1\right). \tag{18}$$

Finally, the total cross section is

$$\sigma_T = \sigma_e + \sigma_{ce} + \sigma_A. \tag{19}$$

Use of this expression brings the total $p\bar{p}$ cross section into good agreement with the experimental data, as can be seen in Fig. 4. This indicates that the real part, which is completely given by the model, should be realistic.

We check the isospin dependence of our $N\bar{N}$ potential by studying the $p\bar{n}$ reaction. Notice that we do not include any isospin dependence in the annihilation potential, so all the isospin dependence comes from the real part of the potential and is fixed from the NN sector. As $p\bar{n}$ is an isospin 1 state, $\sigma_A^{p\bar{n}} = \sigma_A^1$, $\sigma_e^{p\bar{n}} = \sigma_e^1$, and there is no charge exchange reaction. As can be seen in Figs. 5 and 6 the results, given by the solid line, are in agreement with the data for the total and annihilation cross sections, although in both cases there are big uncertainties. The dashed line shows the result for the model [24] that uses an isospin-dependent annihilation potential. Both lines show almost the same agreement with the data. In fact, in the $p_{\rm lab}$ range between 105 and 550 MeV, the χ^2/datum for the total annihilation cross section is 1.09 for our model and 1.26 for the isospin-dependent model, and for the total cross section it is 1.51 for our model and 2.18 for the isospin-dependent model. Notice that these values in our case are not minimized and we only give them as a measure of the agreement with the data.

So we do not find any reason to include an isospin dependence in our optical potential. This fact is consistent with the assumption that the optical potential represents an average effect of numerous annihilation channels, which one would expect to be spin and isospin independent.

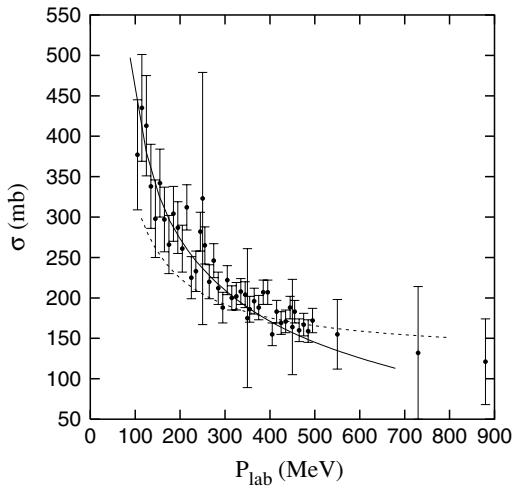

FIG. 5. $p\bar{n}$ total cross section. The solid line corresponds to this work and the dashed line to [24] in which an isospin-dependent annihilation potential is used. Experimental data are from Refs. [30,31].

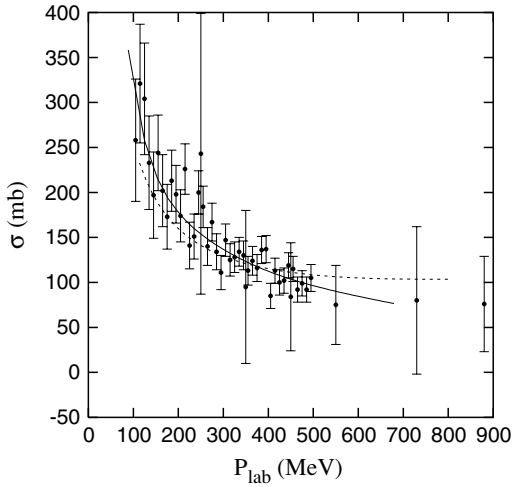

FIG. 6. $p\bar{n}$ annihilation cross section. Lines are the same as in Fig. 5. Experimental data are from Refs. [30,31].

Now we are in the position to study possible $N\bar{N}$ bound states. In the NN sector our model only gives one bound state, which correspond to the deuteron [11]. Now, as we have an imaginary part for the potential, the bound states are transformed into resonances. We solve the Schrödinger equation by allowing complex values for the eigenenergies and so get the mass and width of the states.

If we do not include the imaginary potential, the real part of the potential predicts two bound states. One has quantum numbers $J^{\rm PC} = 1^{--}$, which is a $^3S_1$-$^3D_1$ partial wave in $I = 0$ and the other is $J^{\rm PC} = 0^{++}$, which is a $^3P_0$ state also with $I = 0$. Both states are very close to threshold, being the binding energy 1.30 MeV for the first one and 1.32 MeV for the second one. We find the strongest interactions in S waves with $I = 0$, which is much bigger than for $I = 1$, and for the $^3P_0$ wave for $I = 0$, which is also much bigger than for $I = 1$.

When we include the annihilation potential the 1^{--} state is washed out and the 0^{++} state is transformed in a near-threshold resonance with a mass 18.5 MeV above threshold and a width of 33.6 MeV. In Table II we give the energy eigenvalues of the state for values of W_i from 0 to the realistic $-0.74\,{\rm GeV}^{-2}$. The mass goes above the $N\bar{N}$ threshold for values between -0.14 and -0.24.

TABLE II. Real and imaginary parts of the $^3P_0$ $I = 0$ self-energy as a function of the optical potential strength parameter W_i.

W_i (GeV^{-2})	Re[E] (MeV)	Im[E] (MeV)
−0.00	−1.3	0.0
−0.14	−0.6	−3.2
−0.24	0.8	−5.5
−0.34	2.8	−7.8
−0.44	5.6	−10.2
−0.54	9.0	−12.4
−0.64	13.3	−14.7
−0.74	18.5	−16.8

To see the relative size of the different contributions we switch off the gluon contribution. In this case we still find a resonance with a mass 14.0 MeV above threshold and a width of 80.8 MeV. By removing only the one-pion exchange the resonance disappears.

Our results do not support the hypothesis that the near-threshold enhancement in the $p\bar{p}$ invariant mass spectrum of the radiative decays $J/\psi \to \gamma p\bar{p}$ is due to the presence of a baryonium bound state in the S wave or P wave and therefore other explanations should be considered. These results are consistent with the fact that despite the efforts done at LEAR and other facilities to find indications of $N\bar{N}$ bound states none have been found until now. The only experimental indication of some structure in the $N\bar{N}$ observables is the abnormally large value of the protonium P level in the $^3P_0$ state [32].

V. PROTONIUM ENERGY SHIFTS

The study of antiprotonic atoms offers a chance to test nucleon-antinucleon scattering amplitudes just at threshold. The essential features of antiprotonic atoms can be understood in terms of the electromagnetic interaction, and the energy levels E_n are described by the Bohr formula being a function of the principal quantum number n and proportional to the reduced mass μ. However, the protonium atomic levels are shifted and widened by the strong interaction; that is, the full energy E_{nl} is shifted from the electromagnetic level ϵ_{nl} by a complex level shift $\Delta E_{nl} = E_{nl} - \epsilon_{nl} = \delta E_{nl} - i\Gamma_{nl}/2$. Protonium spectroscopy was actively pursued at LEAR between 1983 and 1996 and determinations were made of the energy shifts and broadenings for the $1s$ and $2p$ levels [33,34]. One of the most interesting outcomes of this experiments is that the $^3P_0$ protonium level shift $\delta E(^3P_0) = -139 \pm 28$ meV is much bigger than any other. This result suggests the existence of a near-threshold $N\bar{N}$ resonance that enhances the scattering amplitude. The energy shifts in hadronic atoms can be determined with the improved Trueman formula, deduced through an analytic continuation of the scattering amplitude [7,35], by using the scattering length (S wave) or the scattering volume (P waves)

$$\delta E_{nl} = -E_n \frac{4}{n} \frac{a_l}{a_B^{2l+1}} \alpha_{nl} \left(1 - \frac{a_l}{a_B^{2l+1}} \beta_{nl} + \ldots \right), \qquad (20)$$

where $a_B = \hbar/\alpha\mu c$ is the Bohr radius of the system, a_l is the scattering length (volume), and α_{nl} and β_{nl} are defined as

$$\alpha_{nl} = \prod_{s=1}^{l} \left(\frac{1}{s^2} - \frac{1}{n^2} \right), \qquad \alpha_{n0} = 1, \qquad (21)$$

$$\beta_{n0} = 2\left[\log n + \frac{1}{n} - \Psi(n) \right], \quad \beta_{n1} = \alpha_{n1}\beta_{n0} - \frac{4}{n^3}, \qquad (22)$$

with Ψ being the digamma function.

An alternative approach is to use perturbation theory, which for weak potentials reproduces the former result [36]. However, it is important to note here that this is not the case for protonium S waves. For these particular waves the strong interaction is big enough compared to the Coulombic one

TABLE III. $p\bar{p}$ energy shifts calculated from the improved Trueman formula (ΔE) and coupled contribution from the Holstein formula (ΔE_c) and from perturbation theory. In the perturbative calculation $\Delta E_{p\bar{p}}$ includes only corrections from $p\bar{p}$ states.

State	a_l (fm^{2l+1})	ΔE	ΔE_c	$\Delta E_{p\bar{p}}$	$\Delta E_{\rm exp}$	
$1\,^1S_0$	$0.61 - i1.01$	$557.3 - i820.9$	$2.3 + i6.5$	$-587.5 - i2263.4$	$440 \pm 75 - \mathrm{i}(600 \pm 125)$[a]	eV
$2\,^1S_0$		$67.7 - i106.3$	$0.1 + i0.4$	$-73.4 - i28.3$		
$2\,^1P_1$	$-1.14 - i0.51$	$-27.9 - i12.4$		$-27.0 - i10.4$		meV
$2\,^3P_0$	$-2.75 - i3.87$	$-67.3 - i94.7$		$-71.8 - i10.4$	$-140 \pm 28 - \mathrm{i}(60 \pm 12)$ [b]	meV
$2\,^3P_1$	$1.49 - i0.44$	$36.5 - i10.9$		$40.1 - i10.4$		meV

[a]Reference [33].
[b]Reference [34].

in its range so that perturbation theory does not work. For P waves the centrifugal barrier contributes to soften the strong interaction, preventing the shorter range contributions, and perturbation theory becomes useful.

We use the improved Trueman formula to calculate the energy shifts and half-width for the $p\bar{p}$ $L = 0$ and $L = 1$ partial waves. The results are shown in Table III. We also include the results of the perturbative calculation for the P waves, which are compatible with the those calculated with the Trueman formula. One can see from this table that the experimental results are well reproduced except for the $^3P_0$ energy shift, which is underestimated by a factor of 2. These predictions coincide basically with those obtained with other potentials [32]. The obtained result for the $^3P_0$ energy shifts is telling us that our one-channel model is too simple. In particular our one-pion exchange piece of the interaction couples the $p\bar{p}$ and $n\bar{n}$ channels and this coupling may have significant influence in the theoretical predictions.

The Trueman formula is not valid for the coupled-channel case but we will use the generalization for the S wave given in Ref. [36]. This gives an additional contribution of

$$\Delta E_c = E_n \frac{4}{n a_B} \frac{i k_1 a'^2}{1 + i k_1 a_l} \tag{23}$$

with $a' = \frac{1}{2}(a_1 - a_0)$ the scattering length for the transition amplitude.

For P waves we use coupled-channel perturbation theory. We start from the coupled equations

$$H_{p\bar{p}}|p\bar{p}\rangle + V_{n\bar{n}\to p\bar{p}}|n\bar{n}\rangle = E|p\bar{p}\rangle, \tag{24}$$

$$H_{n\bar{n}}|n\bar{n}\rangle + V_{p\bar{p}\to n\bar{n}}|p\bar{p}\rangle = E|n\bar{n}\rangle, \tag{25}$$

with

$$H_{p\bar{p}} = \frac{p^2}{2\mu} + V^{\rm em}_{p\bar{p}} + V_{p\bar{p}}, \tag{26}$$

$$H_{n\bar{n}} = \frac{p^2}{2\mu} + V_{n\bar{n}}, \tag{27}$$

$$V_{p\bar{p}} = V_{n\bar{n}} = \tfrac{1}{2}\,(V_1 + V_0)\,, \tag{28}$$

$$V_{p\bar{p}\to n\bar{n}} = V_{p\bar{p}\to n\bar{n}} = \tfrac{1}{2}(V_1 - V_0), \tag{29}$$

where $V^{\rm em}_{p\bar{p}}$ is the electromagnetic interaction and V_1 (V_0) is the strong potential in isospin channel 1 (0). From Eq. (25) we get

$$|n\bar{n}\rangle = \frac{1}{E - H_{n\bar{n}}} V_{p\bar{p}\to n\bar{n}}|p\bar{p}\rangle; \tag{30}$$

inserting it in Eq. (24) we get

$$\left(\frac{p^2}{2\mu} + V^{\rm em}_{p\bar{p}} + V_{p\bar{p}} + V_{n\bar{n}\to p\bar{p}} \frac{1}{E - H_{n\bar{n}}} V_{p\bar{p}\to n\bar{n}}\right) \times |p\bar{p}\rangle = E|p\bar{p}\rangle. \tag{31}$$

So we consider as a perturbation the effective $p\bar{p}$ potential

$$V^{\rm eff}_{p\bar{p}} = V_{p\bar{p}} + V_{n\bar{n}\to p\bar{p}} \frac{1}{E - H_{n\bar{n}}} V_{p\bar{p}\to n\bar{n}}. \tag{32}$$

The unperturbed wave function is the Coulomb wave function $|\psi^{nl}_{p\bar{p}}\rangle$, so the first energy correction is given by

$$\Delta E_{nl} = \left\langle \psi^{nl}_{p\bar{p}} \middle| V^{\rm eff}_{p\bar{p}} \middle| \psi^{nl}_{p\bar{p}} \right\rangle = \Delta E_{p\bar{p}} + \Delta E_{n\bar{n}}, \tag{33}$$

TABLE IV. $p\bar{p}$ energy shifts calculated from perturbation theory. $\Delta E_{p\bar{p}}$ includes only corrections from $p\bar{p}$ states whereas $\Delta E_{n\bar{n}}$ includes corrections from the coupling to $n\bar{n}$ states. $\Delta E_f = \Delta E_{p\bar{p}} + \Delta E_{n\bar{n}}$ is the full result. The last column shows the full result removing the gluon ΔE^g_f and the pion ΔE^π_f contributions.

State	$\Delta E_{p\bar{p}}$	$\Delta E_{n\bar{n}}$	ΔE_f	ΔE^g_f	ΔE^π_f	
$2\,^1P_1$	$-27.0 - i10.4$	$-1.5 - i0.07$	$-28.5 - i10.4$	$-29.2 - i10.4$	$-5.9 - i10.4$	meV
$2\,^3P_0$	$-71.8 - i10.4$	$-40.4 - i15.7$	$-112.2 - i26.0$	$-113.6 - i30.8$	$-5.34 - i10.4$	meV
$2\,^3P_1$	$40.1 - i10.4$	$-10.5 - i1.8$	$29.6 - 12.1$	$28.6 - i12.2$	$-5.34 - i10.4$	meV

with

$$\Delta E_{p\bar{p}} = \langle \psi^{nl}_{p\bar{p}} | V_{p\bar{p}} | \psi^{nl}_{p\bar{p}} \rangle, \tag{34}$$

$$\Delta E_{n\bar{n}} = \langle \psi^{nl}_{p\bar{p}} | V_{n\bar{n}\to p\bar{p}} \frac{1}{E_n - H_{n\bar{n}}} V_{p\bar{p}\to n\bar{n}} | \psi^{nl}_{p\bar{p}} \rangle. \tag{35}$$

Results are shown in Table IV. As we can see the coupling with the $n\bar{n}$ channel has little effect on the energy shift except for the $^3P_0$ partial wave. The observed enhancement in this wave is due to the resonance being located close to the $N\bar{N}$ threshold in this channel.

The last two columns of Table IV show the energy shift without the gluon and pion contribution, respectively. One can see that the main contribution is the one given by the pion.

VI. CONCLUSIONS

We have investigated the possible existence of bound states in the $N\bar{N}$ system and its possible influence in the protonium level shifts. We have built a $N\bar{N}$ potential derived from the Salamanca quark-model-based *NN* potential supplemented by a phenomenological spin- and isospin-independent imaginary part of Gaussian form.

There are three important outcomes of our calculation. First, our model is able to reproduce the isospin dependence of the $N\bar{N}$ cross section without using any additional isospin dependence but the one coming from the real part of the interaction. This part is given by the G-parity transform of the qq interaction and the annihilation diagrams of Fig. 1. Second, our potential does not show any $N\bar{N}$ bound state, only a near-threshold resonance appearing in the $^3P_0$ partial wave, as seems to be required the by phenomenology. Finally, we are able to reproduce the energy level shifts in protonium. In particular we showed that in our model the large $^3P_0$ protonium energy shift can be justified as a combined effect of the $p\bar{p}$ and $n\bar{n}$ coupled channel and the $p\bar{p}$ resonance found at threshold in the $I = 0$ channel.

The discussion of the influence of the $p\bar{p}$ final-state interaction in the observed enhancement in J/ψ decay will be addressed in a forthcoming paper [37].

ACKNOWLEDGMENTS

This work has been partially funded by Ministerio de Ciencia y Tecnologí a under Contract No. FPA2004-05616 and by Junta de Castilla y León under Contract No. SA-104/04.

[1] J. Z. Bai *et al*. (BES Collaboration), Phys. Rev. Lett. **91**, 022001 (2003).
[2] A. Datta and P. J. O'Donnell, Phys. Lett. **B567**, 273 (2003).
[3] C.-H. Chang and H.-R. Pang, Commun. Theor. Phys. **43**, 275 (2005); hep-ph/0407188.
[4] G.-J. Ding and M.-L. Yan, Phys. Rev. C **72**, 015208 (2005).
[5] B. Loiseau and S. Wycech, Phys. Rev. C **72**, 011001(R) (2005).
[6] A. Sibirtsev, J. Haidenbauer, S. Krewald, Ulf-G. Meissner, and A. W. Thomas, Phys. Rev. D **71**, 054010 (2005).
[7] E. Klempt, F. Bradamante, A. Martin, and J.-M. Richard, Phys. Rep. **368**, 119 (2002).
[8] T. Hippchen, J. Haidenbauer, K. Holinde, and V. Mull, Phys. Rev. C **44**, 1323 (1991).
[9] F. Myhrer and A. W. Thomas, Phys. Lett. **B64**, 59 (1976).
[10] F. Fernández, A. Valcarce, P. González, and V. Vento, Phys. Lett. **B287**, 35 (1992).
[11] D. R. Entem, F. Fernández, and A. Valcarce, Phys. Rev. C **62**, 034002 (2000).
[12] A. Valcarce, H. Garcilazo, F. Fernández, and P. González, Rep. Prog. Phys. **68**, 965 (2005); J. Vijande, F. Fernández, and A. Valcarce, J. Phys. G **31**, 481 (2005).
[13] A. Manohar and H. Georgi, Nucl. Phys. **B234**, 189 (1984).
[14] D. Diakonov, Prog. Part. Nucl. Phys. **51**, 173 (2003).
[15] J. W. Durso, A. D. Jackson, and B. J. VerWest, Nucl. Phys. **A345**, 471 (1980).
[16] Y. Tzeng, J. Phys. G **17**, 221 (1991).
[17] S. D. Bass, Phys. Lett. **B463**, 286 (1999).
[18] G. S. Bali, Phys. Rep. **343**, 1 (2001).
[19] A. Faessler, G. Lübeck, and K. Shimizu, Phys. Rev. D **26**, 3280 (1982).
[20] E. Klempt, C. Batty, and J.-M. Richard, Phys. Rep. **413**, 197 (2005).
[21] R. A. Bryan and R. J. Phillips, Nucl. Phys. **B5**, 201 (1968); **B7**, 481 (1968) (erratum).
[22] C. B. Dover and J.-M. Richard, Phys. Rev. C **21**, 1466 (1980); J.-M. Richard and M. E. Saino, Phys. Lett. **B110**, 349 (1982).
[23] M. Kohno and W. Weise, Nucl. Phys. **A454**, 429 (1986).
[24] P. Bydzovsky, R. Mach, and F. Nichitiu, Phys. Rev. C **43**, 1610 (1991).
[25] W. Brückner *et al*., Z. Phys. A **335**, 217 (1990).
[26] T. Kamae *et al*., Phys. Rev. Lett. **44**, 1439 (1980).
[27] K. Nakamura *et al*., Phys. Rev. D **29**, 349 (1984).
[28] A. S. Clough *et al*., Phys. Lett. **B146**, 299 (1984).
[29] D. V. Bugg *et al*., Phys. Lett. **B194**, 563 (1987).
[30] B. Gunderson, J. Learned, J. Mapp, and D. D. Reeder, Phys. Rev. D **23**, 587 (1981).
[31] T. Armstrong *et al*., Phys. Rev. D **36**, 659 (1987).
[32] J. Carbonell and M. Mangin-Brinet, Nucl. Phys. **A692**, 11c (2001).
[33] M. Augsburger *et al*., Nucl. Phys. **A658**, 149 (1999).
[34] D. Gotta *et al*., Nucl. Phys. **A660**, 283 (1999).
[35] T. L. Trueman, Nucl. Phys. **26**, 57 (1961).
[36] B. R. Holstein, Phys. Rev. D **60**, 114030 (1999).
[37] D. R. Entem and F. Fernández, in preparation.